

# Display Technology Letters

## Fast-Response Single Cell Gap Transflective Liquid Crystal Displays

Meizi Jiao, Shin-Tson Wu, *Fellow, IEEE*, and Wing-Kit Choi

**Abstract**—A single cell gap transflective liquid crystal display (TR-LCD) using dual fringing field switching mode is proposed, in which a positive dielectric anisotropy liquid crystal is vertically aligned and driven by fringing fields from both substrates. By optimizing the electrode width and gap of the transmissive and reflective regions, this TR-LCD exhibits a fast response time, high optical efficiency, single gamma curve, and wide viewing angle. Fast response time enables color sequential operation using red, green, and blue light-emitting diodes without noticeable color breakup. Potential application of this TR-LCD for sunlight readable mobile displays is emphasized.

**Index Terms**—Transflective liquid crystal displays (TR-LCDs), fast response, single cell gap, color sequential display.

### I. INTRODUCTION

WIDE-VIEW transflective liquid crystal displays (TR-LCDs) [1], [2] have been widely used in mobile displays, such as digital cameras, portable video players, and cell phones because of their sunlight readability and low power consumption. Wide-view TR-LCDs can be achieved by using fringing field switching (FFS) [3], [4] or multi-domain vertical alignment (MVA) [5]–[7], while low power consumption can be obtained by improving optical efficiency or using sequential colors. In a color sequential LCD [8], the color filters can be eliminated so that the optical efficiency and device resolution are tripled. However, to achieve color sequential without causing noticeable color break-up requires LC's response time to be shorter than 3 ms.

A major challenge for TR-LCD is to balance the phase retardation between the transmissive (T) and reflective (R) sub-pixels. In the T region, the backlight traverses the LC layer once, but in the R region the ambient light passes through the LC layer twice. To balance this optical path-length disparity, various dual cell gap and single cell gap approaches have been proposed. Single cell gap approach is more favorable because it is easier to

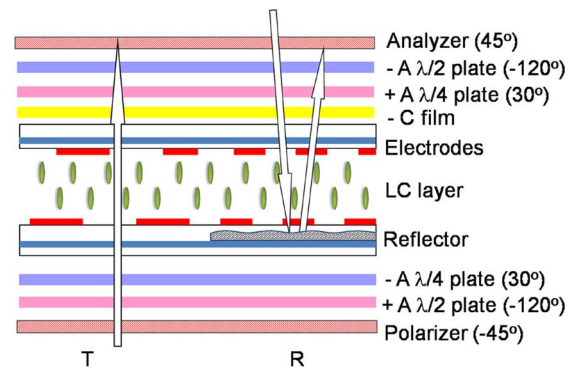


Fig. 1. Schematic structure of the single cell gap TR-LCD using DFFS mode.

fabricate, however, it is more difficult to achieve the same phase retardation than the dual cell gap approach.

In this letter, we propose a single cell gap TR-LCD using a dual fringing field switching (DFFS) effect. A positive dielectric anisotropy ( $\Delta\epsilon > 0$ ) LC is employed in a VA cell. Driven by the fringing fields near the substrate surface, a two-domain profile is formed without any protrusion or rubbing process [9]. From our simulations, the TR-LCD exhibits a fast response time with a maximum transmittance  $\sim 95.4\%$  and reflectance  $\sim 93.8\%$ , as normalized to the transmittance of two parallel polarizers. By using different electrode width and gap in the T and R regions, the voltage-dependent transmittance (VT) and reflectance (VR) curves overlap fairly well. This is useful for single gamma curve driving. With proper phase compensation, the TR-LCD also exhibits a reasonably wide viewing angle.

### II. DEVICE CONFIGURATION

Fig. 1 shows a cross section of the schematic structure of the proposed TR-LCD using the DFFS mode in the voltage-off state. A positive  $\Delta\epsilon$  LC is initially aligned in a VA cell. On each side of the LC cell, a broadband quarter-wave plate [10] together with a linear polarizer works as a circular polarizer. Additionally, one negative C-film is adopted to compensate the phase retardation from the VA LC cell. On each substrate, the electrode has the same structure as the conventional FFS LCD which has a planar common electrode and stripe pixel electrodes [11], [12]. The top and bottom pixel electrodes are intentionally registered by shifting one half a pixel electrode width in the horizontal direction to create complementary domains on two opposite sides to enhance the optical efficiency and spatial uniformity.

Each display pixel is divided into T and R two sub-pixels [2]. To obtain the same on-state phase retardation between the T and

Manuscript received October 17, 2008; revised November 24, 2008. Current version published February 19, 2009. This work was supported by Chi-Mei Optoelectronics Corporation (Taiwan).

M. Jiao and S. T. Wu are with the College of Optics and Photonics, University of Central Florida, Orlando, FL 32816 USA (e-mail: mjiao@mail.ucf.edu; swu@mail.ucf.edu).

W.-K. Choi is with Graduate Institute of Photonics and Optoelectronics, National Taiwan University, Taipei 10617, Taiwan (e-mail: wkchoi@cc.ee.ntu.edu.tw).

Color versions of one or more figures are available online at <http://ieeexplore.ieee.org>.

Digital Object Identifier 10.1109/JDT.2009.2012394

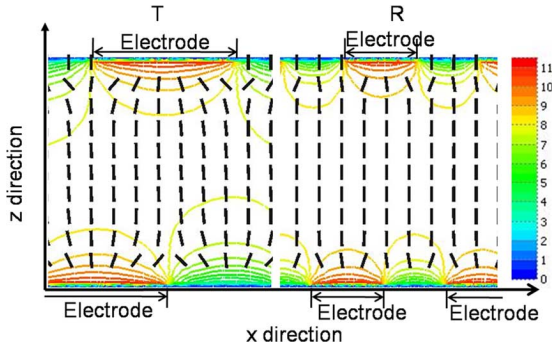


Fig. 2. Equal-potential line distribution in the LC cell for a sample section with 11  $V_{rms}$  applied to pixel electrode. Cell gap  $d = 14 \mu\text{m}$ ; T part: electrode width  $W = 3.2 \mu\text{m}$ , electrode gap  $G = 3.2 \mu\text{m}$ ; R part:  $W = 2 \mu\text{m}$  and  $G = 2 \mu\text{m}$ .

R regions, we design the electrode width ( $W$ ) and electrode gap ( $G$ ) in the R region to be smaller than those in the T region. Therefore, the LC director reorientation-induced effective birefringence in the R region ( $(\Delta n)_R$ ) is smaller than that in the T region ( $(\Delta n)_T$ ). Our goal is to achieve  $(\Delta n)_R \sim (\Delta n)_T/2$  so that the total phase retardation in the R and T regions are approximately equal, i.e.,  $2d(\Delta n)_R \sim d(\Delta n)_T$ .

### III. RESULT

The proposed TR LCD structure is optimized using a commercial three-dimensional LC simulator (TECHWIZ developed by Sanayi). The LC distribution is calculated by the finite-element method [13] and the optical properties are calculated based on extended  $2 \times 2$  Jones matrix methods [14], [15]. The LC material used in simulation is Merck E7 with parameters as follows:  $K_{11} = 11.7 \text{ pN}$ ,  $K_{22} = 8.8 \text{ pN}$ ,  $K_{33} = 19.5 \text{ pN}$ , birefringence  $\Delta n = 0.223$ , dielectric anisotropy  $\Delta \epsilon = 14.4$ , and rotational viscosity  $\gamma_1 = 250 \text{ mPa}\cdot\text{s}$ . Merck E7 is used here as an example to show the optical performances of the proposed TR LCD. Some isothiocyanato-biphenyl LC mixtures with similar birefringence but with a lower viscosity ( $\gamma_1 < 100 \text{ mPa}\cdot\text{s}$ ) have been developed [16]. A lower viscosity leads to a faster response time. In our calculations, the cell gap is  $d = 14 \mu\text{m}$ , electrode width  $W = 3.2 \mu\text{m}$  and electrode gap  $G = 3.2 \mu\text{m}$  for the T region, and  $W = 2 \mu\text{m}$  and  $G = 2 \mu\text{m}$  for the R region.

Fig. 2 shows the calculated equal-potential line distribution when the same pixel voltage of 11  $V_{rms}$  is applied to both T region and R region. The potential difference between two neighboring potential lines is  $0.5 V_{rms}$ . The strong fringing field is mainly confined to the electrode surfaces, thus, only the boundary LC directors are perturbed by the strong horizontal fields while the middle LC layer remains as a standing layer. Because R region has narrower electrode width and electrode gap than T region, the strong fringing fields penetrate to a thinner LC layer in the R region, resulting in a smaller effective birefringence than the T region. This is actually desirable because ambient light passes through R region twice but backlight passes T region only once. As stated earlier, the ideal case is to obtain  $(\Delta n)_R \sim (\Delta n)_T/2$ .

Fig. 3 shows the simulated VT and VR curves. Here the maximum transmittance from two parallel linear polarizers in our simulation is  $\sim 37\%$ . And the effective peak transmittance and reflectance of the proposed TR-LCD reach  $\sim 95.4\%$  and  $93.8\%$ , respectively. The inset in Fig. 3 shows the normalized

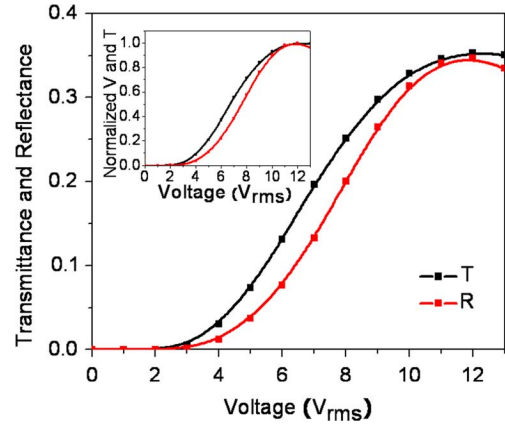


Fig. 3. VT and VR curves for the proposed TR-LCD. The inset shows the normalized results.

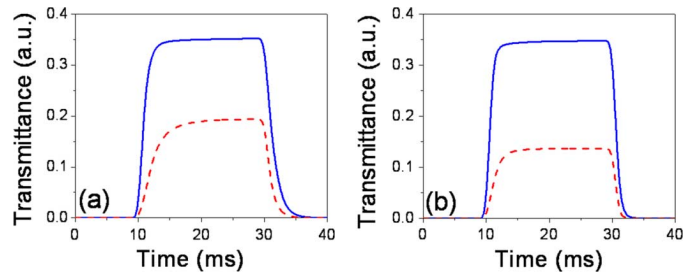


Fig. 4. Simulated response times for the proposed TR-LCD, (a) transmissive part and (b) reflective part, solid lines for black-white transition and dash lines for mid-gray level transition.

VT and VR curves. We find that T region and R region have the same on-state voltage ( $\sim 12 V_{rms}$ ) and a very similar threshold voltage ( $\sim 2.5 V_{rms}$ ). The VT and VR curves overlap fairly well which makes it possible for a single gamma driving. As noted from Fig. 3, the driving voltage of this TR-LCD is still too high. To lower the on-state voltage, we could continue to optimize the device structure or use a higher  $\Delta \epsilon$  LC material, such as (3,5) difluoro NCS-biphenyl LC mixture. The NCS-biphenyl compounds exhibit a high birefringence, large dielectric anisotropy ( $\Delta \epsilon \sim 12$ ), and relatively low viscosity, however, their resistivity is not high enough for thin film transistor (TFT) LCD applications. The (3,5) fluoro groups not only increase dielectric anisotropy to  $\Delta \epsilon \sim 20$  but also dramatically boost resistivity [17]. High resistivity is important for TFT LCD devices in order to avoid image flickering.

The response time (10%–90% transmittance change) of the TR-LCD is calculated as plotted in Fig. 4(a) for T part and Fig. 4(b) for R part. The rise time and decay time for T part is  $\sim 1.8 \text{ ms}$  and  $\sim 2.9 \text{ ms}$ , while for R part they are  $\sim 1.1 \text{ ms}$  and  $\sim 1.3 \text{ ms}$ , respectively, as shown by the blue color. Furthermore, the response time at a middle gray level ( $V = 7 V_{rms}$ ) is also included (red dashed lines) in Fig. 4 to illustrate the gray-to-gray (GTG) transition. For the T part, the simulated [rise, decay] time is  $[\sim 5.1, \sim 2.1] \text{ ms}$ , and  $[\sim 2.7, \sim 0.9] \text{ ms}$  for the R part, respectively. These response times are obtained in an E7 LC cell without using any overdrive voltage. The fast response time makes this TR-LCD attractive for color sequential displays.

Three factors contribute to the observed fast response time: Firstly, the thick cell forms a vertical wall separating the two thin LC cells near the top and bottom surfaces. Even at an on-state,

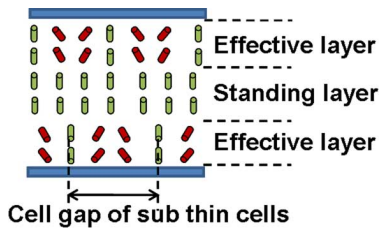


Fig. 5. Illustration of on-state LC distribution.

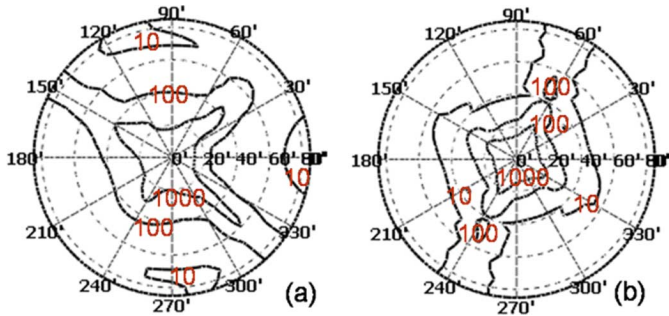


Fig. 6. Iso-contrast contour plot of the TR-LCD with compensation films: (a) for transmissive part and (b) for reflective part.

the electric field in the middle of the cell is too weak to rotate the LC directors. Therefore, the LC layer is divided into two effective layers and one standing layer in between, as shown in Fig. 5. The LC layer thickness for the effective layers is actually very small. Secondly, domain walls are formed in the horizontal direction and separate the effective layers into sub thin cells in horizontal direction, as shown in Fig. 5. These domain walls also supply a restoring force during switching-off process. And thirdly, the on-state LC profile between two horizontal walls is similar to a bend cell [18], where the LC flow effect in DFFS helps LC directors switch faster.

The DFFS cell does not require any rubbing process. The LC directors form two domains on both LC boundary layers due to the fringing field effect. If zigzag electrodes are employed, then a four-domain structure is produced which leads to a wide viewing angle. As shown in Fig. 1, on each side of the LC cell, together with a linear polarizer, +A and -A plates are used alternately as half-wave plate (HWP) and quarter-wave plate (QWP) to form a self-compensated wideview and broadband circular polarizer [10], [19]. An additional -C plate is used to compensate the viewing angle properties of the TR-LCD under circular polarizer system. The parameters of the compensation films used in our simulation are listed as follows: For +A plate,  $n_e = 1.65, n_o = 1.55$ ; for -A plate,  $n_e = 1.55, n_o = 1.65$ ; for -C plate,  $n_e = 1.55, n_o = 1.65$  and its thickness  $d = 29.26 \mu\text{m}$ . The thicknesses of the HWP and QWP are  $2.75 \mu\text{m}$  and  $1.375 \mu\text{m}$ , respectively. With the transmission axis of polarizer and analyzer orientated at  $-45^\circ$  and  $45^\circ$ , respectively, the optic axis of HWP and QWP are orientated at  $-120^\circ$  and  $30^\circ$  on each side of the LC cell.

Fig. 6 shows the iso-contrast contour after phase compensation. T part shows a contrast ratio 10:1 over  $\sim 70^\circ$  viewing cone and R part over  $\sim 40^\circ$ . These viewing angles are adequate for most mobile displays. A hand-held LCD is usually viewed by only one person.

#### IV. CONCLUSION

In conclusion, we have proposed a single cell gap TR-LCD using DFFS mode. This device shows a fast response without using thin cell gap approach or overdrive method. This makes it a promising candidate for color sequential displays. Its optical efficiencies are over 90% for both T part and R part and will even be increased to  $\sim 3X$  if color sequential method is adopted. As the energy problem of the world has become more and more serious, such an energy-effective TR-LCD is foreseeable to have a lot of potential applications.

#### REFERENCES

- [1] S. T. Wu and D. K. Yang, *Reflective Liquid Crystal Displays*. Hoboken, NJ: Wiley, 2001.
- [2] X. Zhu, Z. Ge, T. X. Wu, and S. T. Wu, "Transflective liquid crystal displays," *J. Display Technol.*, vol. 1, no. 1, pp. 15–29, Sep. 2005.
- [3] J. H. Lee, X. Zhu, and S. T. Wu, "Novel color-sequential transflective liquid crystal displays," *J. Display Technol.*, vol. 3, no. 1, pp. 2–8, Mar. 2007.
- [4] T. B. Jung, J. C. Kim, and S. H. Lee, "Wide-viewing-angle transflective display associated with a fringe-field driven homogeneously aligned nematic liquid crystal display," *Jpn. J. Appl. Phys.*, vol. 42, pp. 464–467, 2003.
- [5] H. Y. Kim, Z. Ge, and S. T. Wu, "Wide-view transflective liquid crystal display for mobile applications," *Appl. Phys. Lett.*, vol. 91, p. 231108, 2007.
- [6] S. H. Lee, H. W. Do, G. D. Lee, T. H. Yoon, and J. C. Kim, "A novel transflective liquid crystal display with a periodically patterned electrode," *Jpn. J. Appl. Phys.*, vol. 42, pt. 2, pp. L1455–L1458, 2003.
- [7] Y. J. Lee, T. H. Lee, J. W. Jung, H. R. Kim, Y. Choi, S. G. Kang, Y. C. Yang, S. Shin, and J. H. Kim, "Transflective liquid crystal display with single cell gap in patterned vertically aligned mode," *Jpn. J. Appl. Phys.*, vol. 45, pp. 7827–7830, 2006.
- [8] C. H. Lin, Y. R. Chen, S. C. Hsu, C. Y. Chen, C. M. Chang, and A. Lien, "A novel advanced wide-view transflective display," *J. Display Technol.*, vol. 4, no. 2, pp. 123–128, Jun. 2008.
- [9] M. Jiao, Z. Ge, S. T. Wu, and W. K. Choi, "Submillisecond response nematic liquid crystal modulators using dual fringe field switching in a vertically aligned cell," *Appl. Phys. Lett.*, vol. 92, p. 111101, 2008.
- [10] C. Z. Xiang, X. W. Sun, and X. Y. Jin, "Fast response wide viewing angle liquid crystal cell with double-side fringe-field switching," *Appl. Phys. Lett.*, vol. 83, pp. 5154–5156, 2003.
- [11] H. Y. Kim, G. R. Jeon, D. S. Seo, M. H. Lee, and S. H. Lee, "Dual domain effects on a homogeneously aligned nematic liquid crystal cell driven by a fringe-field," *Jpn. J. Appl. Phys.*, vol. 41, pt. 1, pp. 2944–2948, 2002.
- [12] Z. Ge, M. Jiao, R. Lu, T. X. Wu, S. T. Wu, W. Y. Li, and C. K. Wei, "Wide-view and broadband circular polarizers for transflective liquid crystal displays," *J. Display Technol.*, vol. 4, no. 2, pp. 129–138, Jun. 2008.
- [13] Z. Ge, T. X. Wu, R. Lu, X. Zhu, Q. Hong, and S. T. Wu, "Comprehensive three-dimensional dynamic modeling of liquid crystal devices using finite element method," *J. Display Technol.*, vol. 1, no. 2, pp. 194–206, Dec. 2005.
- [14] A. Lien, "Extended Jones matrix representation for the twisted nematic liquid-crystal display at oblique incidence," *Appl. Phys. Lett.*, vol. 57, pp. 2767–2769, 1990.
- [15] Z. Ge, T. X. Wu, X. Zhu, and S. T. Wu, "Reflective liquid-crystal displays with asymmetric incident and exit angles," *J. Opt. Soc. Amer. A.*, vol. 22, pp. 966–977, 2005.
- [16] R. Dabrowski, "Isothiocyanates and their mixtures with a broad range of nematic phase," *Mol. Cryst. Liq. Cryst.*, vol. 191, pp. 17–27, 1990.
- [17] I. K. Huh and Y. B. Kim, "Fluoro-isothiocyanated liquid crystal materials with high dielectric anisotropy and voltage holding ratio," *Jpn. J. Appl. Phys.*, vol. 41, pt. 1, pp. 6466–6470, 2002.
- [18] P. J. Bos and K. R. Koehler/Beran, "The pi-Cell: A fast liquid-crystal optical-switching device," *Mol. Cryst. Liq. Cryst.*, vol. 113, pp. 329–339, 1984.
- [19] T. H. Yoon, G. D. Lee, and J. C. Kim, "Nontwist quarter-wave liquid-crystal cell for a high-contrast reflective display," *Opt. Lett.*, vol. 25, pp. 1547–1549, 2000.